Title:

microRNA-148a-3p regulates immunosuppression in DNA mismatch repair-deficient colorectal cancer by targeting PD-L1

Authors and affiliations:

Mai Ashizawa[1], Hirokazu Okayama[1], Teruhide Ishigame[2], Aung Kyi Thar Min[1], Katsuharu Saito[1], Daisuke Ujiie[1], Yuko Murakami[3], Tomohiro Kikuchi[1], Masaru Noda[3], Takeshi Tada[1], Hisahito Endo[1], Shotaro Fujita[1], Wataru Sakamoto[1], Motonobu Saito[1], Zenichiro Saze[1], Tomoyuki Momma[1], Shinji Ohki[1], Kosaku Mimura[1,4,5] and Koji Kono[1]

[1]Department of Gastrointestinal Tract Surgery, [2]Department of Hepato-Biliary-Pancreatic and Transplant Surgery, [3]Departmet of Breast Surgery, [4]Department of Advanced Cancer Immunotherapy, [5]Department of Progressive DOHaD Research, Fukushima Medical University School of Medicine, Japan

Running title:

miR-148a-3p regulates PD-L1 in dMMR CRC

Keywords:

Colorectal cancer, microRNA, immune checkpoint

Additional information:

This work was supported by JSPS KAKENHI Grant Numbers 16K07146 and 16K10545. Hirokazu Okayama was supported by The Uehara Memorial Foundation.

Correspondence: Hirokazu Okayama, M. D., Ph. D.
Department of Gastrointestinal Tract Surgery, Fukushima Medical University School of Medicine
1 Hikarigaoka, Fukushima city, Fukushima, 960-1295, Japan.
TEL: +81-24-547-1259
FAX: +81-24-547-1980
E-mail: okayama@fmu.ac.jp

The authors declare no conflicts of interest associated with this manuscript.

Translational Relevance

Programmed cell death 1 (PD-1)/programmed cell death ligand 1 (PD-L1) immune checkpoint blockade has emerged as a promising therapeutic strategy for colorectal cancer (CRC) with microsatellite instability-high (MSI-H) or mismatch repair deficient (dMMR), in which PD-L1 expression is frequently upregulated. Using comprehensive miRNA screening of 260 tumors combined with sequence-based target prediction algorithms, we identified a tumor suppressive miRNA, miR-148a-3p as a potential negative regulator of PD-L1 expression by targeting the 3'-untranslated region (UTR) of PD-L1 mRNA, particularly in dMMR/MSI-H CRC. Forced expression of miR-148a-3p in CRC cell lines suppressed IFN-γ-induced PD-L1 expression on tumor cell surface and consequently reduced apoptotic cell death in co-cultured T-cells. Our findings provide novel evidence that miR-148a-3p regulates immune evasion via PD-L1 and may guide development of novel cancer biomarkers as well as therapeutic interventions for CRC.

Abstract

Purpose: Immunotherapy against the interaction between programmed cell death 1 (PD-1)/programmed cell death ligand 1 (PD-L1) has emerged as a promising strategy for mismatch repair deficient (dMMR) colorectal cancer (CRC). The study aimed to identify microRNAs (miRNAs) that post-transcriptionally control PD-L1 expression on tumor cells and immune evasion, particularly in dMMR CRC.

Experimental Design: A comprehensive miRNA screening was conducted using The Cancer Genome Atlas (TCGA) dataset (n=260) combined with eight different miRNA target prediction programs. Association of miR-148a-3p expression with PD-L1 and MMR status was analyzed in multiple cohorts, including TCGA data, a microarray dataset (n=148), and formalin-fixed paraffin-embedded (FFPE) samples (n=395) by immunohistochemistry and qRT-PCR. Luciferase reporter assays, qRT-PCR, western blotting, and flow cytometry were conducted using HCT116 and SW837 cell lines transfected with miR-148a-3p mimic or inhibitor to confirm the direct regulation of PD-L1. A co-culture model of IL-2-activated T-cells and interferon-γ (IFN-γ)-treated tumor cells was used to investigate the role of miR-148a-3p in T-cell apoptosis via inhibition of tumor cell PD-L1.

Results: The expression of miR-148a-3p was decreased in dMMR tumors, correlating inversely with PD-L1 levels. miR-148a-3p directly binds to the 3'-untranslated region of PD-L1, thereby reducing whole-cell and cell surface PD-L1 levels. Overexpression of miR-148a-3p not only exerted tumor suppressive functions but also repressed IFN-γ-induced PD-L1 expression. Furthermore, T-cell apoptosis was diminished by co-culturing T-cells with cancer cells overexpressing miR-148a-3p.

Conclusions: Our data support a novel regulatory mechanism of PD-L1 expression on tumor cells and immune suppression via miR-148a-3p downregulation in CRC.

Introduction

Despite major advances in diagnosis and treatment, colorectal cancer (CRC) remains the major cause of cancer-death worldwide (1). CRC is commonly grouped into two categories: approximately 15% of tumors with microsatellite instability-high (MSI-H), caused by defective function of the DNA mismatch repair (MMR) system, and the remaining 85% tumors that are microsatellite stable (MSS) exhibiting chromosomal instability (2, 3). Deficient MMR (dMMR) causes the accumulation of many insertion or deletion mutations at microsatellites spread along the genome and produces mutation-induced frameshift peptides (neoantigens), resulting in a high antigen-presenting ability (4, 5). Hence, dMMR cancers are highly immunogenic and thus exhibit a high density of tumor infiltrating lymphocytes (TILs) in the tumor

microenvironment (4, 6). However, concomitant expression of multiple immune checkpoint molecules, including programmed cell death 1 (PD-1) and programmed cell death ligand 1 (PD-L1, also known as B7-H1 and CD274), was demonstrated selectively in dMMR CRC that may counteract the antitumoral immune responses, thereby dMMR cancer cells can evade immune eradication by TILs (6).

Immunotherapy with antibodies blocking the interaction between PD-1 and PD-L1 has emerged as a promising therapeutic strategy in various types of cancer. Although initial studies of immune checkpoint blockade against the PD-1/PD-L1 axis in CRC were not especially promising (7), recent clinical trials have revealed that the anti-PD-1 treatment with pembrolizumab or nivolumab resulted in considerable clinical benefit in patients with dMMR/MSI-H CRC (8, 9).

PD-L1 is expressed on the surface of immune cells and antigen-presenting cells (APCs), and is often upregulated in tumor cells. PD-1 expressed on TILs and its ligand PD-L1 interaction inhibits the effector phase of CD8 cytotoxic T-cell function through T-cell apoptosis and exhaustion (10-12). Transcriptional upregulation of PD-L1 in tumor cells can be induced in response to inflammatory cytokines, such as interferon-γ (IFN-γ) secreted by TILs (12, 13), while it can also be intrinsically driven by oncogenic pathway activation (14, 15). Several post-translational mechanisms to stabilize PD-L1 protein have recently been proposed (16-18). Although multiple pathways can contribute to the expression and function of PD-L1 involved in immune suppression, the detailed understanding of the upregulation of PD-L1 in tumor is limited.

MicroRNAs (miRNAs) are a class of small (18 to 25 nucleotides), non-coding RNA molecules that post-transcriptionally regulate gene expression by binding to the 3'-untranslated region (3'-UTR) of protein-coding mRNAs with imperfect complementarity, leading to translational repression or cleavage of transcripts (19). Altered expression of miRNAs with oncogenic or tumor suppressive functions have been extensively studied in various malignancies (19). Notably, recent studies have demonstrated that several miRNAs expressed in immune cells or cancer cells are crucially involved in cancer-related immune responses by targeting immunosuppressive or immunostimulating factors (20). Moreover, miRNAs may also regulate genes encoding immune checkpoint molecules, including PD-L1 (14). In non-small cell lung cancer (NSCLC), miR-200/ZEB1 axis could control tumor cell PD-L1 expression, linking to an epithelial-mesenchymal transition (EMT) program to increase metastasis (21), and a tumor suppressive miRNA, miR-34 was shown to directly target PD-L1 mRNA (22).

Despite growing evidence that upregulated PD-L1 in tumor cells plays a key role in immune evasion particularly in dMMR CRC, post-transcriptional mechanisms controlling PD-L1 expression and consequent T-cell dysfunction in CRC are not fully understood. Here we hypothesize that miRNAs are involved in the immunosuppressive microenvironment in dMMR CRC via suppression of PD-L1

expression. Using comprehensive miRNA screening combined with sequence-based target prediction algorithms, we identified a tumor suppressive miRNA, miR-148a-3p as a potential regulator of PD-L1 in dMMR CRC. We demonstrate that miR-148a-3p plays an important role in modulating PD-L1 expression that can functionally affect T-cell apoptosis.

Materials and Methods

TCGA data analysis

Level 3 TCGA data for colon adenocarcinoma (COAD), including *CD274* (PD-L1) expression (Illumina RNA-Seq), miRNA expression profiles (Illumina HiSeq) and MMR status based on MSI testing (MSI-High, MSI-Low and microsatellite-stable), were obtained through the TCGA website (https://cancergenome.nih.gov/) (2) and cBioPortal for Cancer Genomics (http://www.cbioportal.org/) in March 2016 (23). Association of miRNA expression with PD-L1 expression or with MMR status were analyzed by BRB-ArrayTools (http://brb.nci.nih.gov/BRB-ArrayTools.html) using correlation analysis or class comparison analysis.

Microarray data analysis

We utilized microarray gene expression and miRNA expression profiles from 148 patients with microsatellite stable (MSS) CRC (24). These datasets are publicly available from the Gene Expression Omnibus (GEO) database (http://www.ncbi.nlm.nih.gov/geo), deposited as GSE81980 based on Affymetrix Human Genome U133 Plus 2.0 array, and GSE81981 based on Agilent-070156 Human miRNA array. The normalized expression values were obtained from each dataset and were not processed further. If a gene or miRNA is represented by multiple probe sets, the expression values of multiple probes were averaged.

miRNA Target prediction

To screen potential miRNAs that potentially bind to the 3'-UTR of *CD274*, we employed 8 target prediction programs, including miRMap (http://mirmap.ezlab.org/), RNA22 (https://cm.jefferson.edu/rna22/), PITA (https://genie.weizmann.ac.il/pubs/mir07/mir07_data.html), miRanda (www.microrna.org), Targetscan (www.targetscan.org), microT-CDS (http://diana.imis.athena-innovation.gr/DianaTools/index.php?r=microT_CDS/), miRWalk (http://www.umm.uni-heidelberg.de/apps/zmf/mirwalk/), and miRDB (www.mirdb.org/miRDB/).

Patient samples

We obtained formalin-fixed paraffin-embedded (FFPE) tissue samples from 395 consecutive patients with primary CRC, who had undergone surgical resection without preoperative chemotherapy or radiotherapy between 1990 and 2013 in Fukushima Medical University (FMU) Hospital. All 395 samples were used for immunohistochemistry (IHC) and 72 samples of them were used for qRT-PCR. The study was conducted in accordance with the Declaration of Helsinki and was approved by the Institutional Review Board of Fukushima Medical University.

Immunohistochemistry (IHC)

For PD-L1 staining, rabbit monoclonal antibody against PD-L1 (#13684, PD-L1 (E1L3N®) XP®, Cell Signaling Technology, Danvers, MA, USA) was used (18, 25-29). Four-μm thick sections were deparaffinized, rehydrated, and endogenous peroxidases were blocked with 0.3% hydrogen peroxide in methanol. Antigens were retrieved by autoclave for 10 min in Tris-EDTA Buffer solution (120℃, pH9.0). The primary antibody was incubated in 1:400 dilution of 10mM phosphate-buffered saline (PBS) containing Tween 20 (Sigma-Aldrich) at 4℃ overnight, and subsequently detected by a horseradish peroxidase (HRP)-coupled anti-rabbit polymer (Envision+System-HRP, Dako, Glostrup, Hovedstaden, Denmark). Sections were then incubated with DAB (Dako), before counterstaining with hematoxylin. Negative controls were done by replacing primary antibody with PBS. Several carcinoma tissues from lung, esophagus, breast, and stomach were used as positive controls. Tumor specimens were considered PD-L1-positive when more than 5% of tumor cells showed membranous staining of any intensity with or without cytoplasmic staining (25, 27, 28).

IHC for MMR proteins including MLH1, MSH2, MSH6, and PMS2 was performed using Dako EnVision+ System with mouse or rabbit monoclonal antibodies against MLH1 (clone ES05, 1:50; Dako), MSH2 (clone FE11, 1:50; Dako), MSH6 (clone EP49, 1:200; Dako) and PMS2 (clone EP51, 1:50; Dako), as described elsewhere (30). Loss of a MMR protein was defined as the absence of nuclear staining of tumor cells in the presence of positive nuclear staining in internal controls.

Determination of MMR status

Tumors demonstrating MSI-H or loss of at least one MMR protein were collectively designated as dMMR, and tumors with non-MSI-H or intact MMR protein expression as proficient MMR (pMMR) (30).

Cell culture

The human CRC cell lines, including SW837 and HCT116, were obtained from JCRB Cell Bank (Osaka, Japan) and RIKEN Cell bank (Ibaraki, Japan), respectively, and were used within 6 months of culture after they were received. Both cell lines were grown in RPMI-1640 (ThermoFisher Scientific, Waltham, MA, USA) containing 10% fetal bovine serum (FBS) and penicillin/streptomycin（100 IU/ml） (ThermoFisher Scientific). Cells were cultured at 37℃ and 5%CO_2 in tissue culture incubator.

Transfection

During the exponential growth phase, cells were transiently transfected with 30nM of mirVana miR-148a-3p Mimic (ID:MC10263), mirVana miR-148a-3p Inhibitor (ID:MH10263), mirVana miRNA Mimic Negative Control#1, or mirVana miRNA Inhibitor Negative Control#1, using Lipofectamine RNAiMAX Reagent (ThemoFisher Scientific) according to the manufacture's protocol. Following 48 hours of incubation, cells were used for each experiment.

Luciferase reporter assay

Complementary 38-bp DNA oligonucleotides containing the putative miR-148a-3p binding site in the 3'-UTR of human *CD274* (antisense: 5'-ctcctagtGTTCCATTTTCAGTGCTTGGGCaagcttgg; sense: 5'-ccaagcttGCCCAAGCACTGAAAATGGAACactaggag-3') were synthesized (PD-L1 wt), and complementary 38-bp DNA oligonucleotides containing mutant 3'-UTR (GCACTG to GCAGAC) were also synthesized as mutant controls (PD-L1 mut). HindⅢ and Spe Ⅰ restriction sites were inserted at both ends of the oligonucleotides. The sense and antisense strands were annealed by adding 1000 ng of each oligonucleotide to 50 μl of 1×NEBuffer 4 (NEB) at 90℃ for 10 min and then at 37℃ for 1 h, and then digested with HindⅢ and SpeI. The annealed oligonucleotides were ligated into the pMIR-REPORT luciferase vector (Ambion, Austin, TX, USA). Three-hundred ng of each reporters were co-transfected with 30nM of miR-148a-3p mimic or negative control into HCT116 cells in 24-well plates. pRL-TK (Promega Corporation, Madison, WI, USA) was used as an internal control. Forty-eight hours after transfection, dual-luciferase activity was assessed with the Dual-Luciferase Reporter Assay system (Promega). Luciferase activity was normalized to internal control according to the manufacturer's specification.

IFN-γ treatment

Twenty-four hours before treatment, tumor cells were transfected with 30nM of mirVana miR-148a-3p mimic or negative control. Then, cells were treated with 10 ng/ml of IFN-γ (Recombinant Human IFN-γ; R&D Systems, Minneapolis, USA) (31). Cells were harvested 48 hours after treatment initiation

and used for each experiment.

RNA extraction

Total RNA from cultured cells was isolated using TRIzol Reagent (ThermoFisher Scientific) according to the manufacturer's instruction. For isolation of total RNA from tissue samples, 72 FFPE tumor specimens were obtained, as described above, including 8 dMMR/PD-L1-positive, 16 pMMR/PD-L1-positive and 48 pMMR/PD-L1-negative patients. Unstained FFPE blocks were marked for carcinoma area and each marked area was macrodissected and selectively sliced into 5 to 10 μm-sections for RNA isolation. RecoverAll Total Nucleic Acid Isolation Kit (ThermoFisher Scientific) was used following the manufacturer's protocol. Isolated total RNA was quantified by NanoDrop.

Quantitative reverse-transcription (qRT)-PCR

For the expression of PD-L1, one-μg of total RNA was reverse transcribed to cDNA using the SuperScript III First-Strand Synthesis System (ThermoFisher Scientific) and qRT-PCR was conducted using TaqMan assays with TaqMan Gene Expression Master Mix (ThermoFisher Scientific) on the 7500 real time PCR system in triplicate. Relative expression levels were determined with SDS software by the $2^{-\Delta\Delta Ct}$ method as described by the manufacturer, with ACTB used as the calibrator gene. The expression levels of mature miRNAs were analyzed using TaqMan MicroRNA Reverse Transcription Kit according to the manufacturer's instruction. Briefly, 40-ng of total RNA was reverse transcribed using miRNA specific RT primers and PCR was performed using TaqMan MicroRNA Assays with the 7500 real time PCR system in triplicate. We used small nuclear RNAs, including RNU66 (for CRC cell lines) or RNU48 (for patient's samples), as endogenous normalization controls. Relative expression levels were determined by the $2^{-\Delta\Delta Ct}$ method. All TaqMan probes were purchased from ThermoFisher Scientific; *CD274* (Hs01125391_m1), *ACTB* (Hs99999903_m1), hsa-miR148a-3p (ID: 000470), RNU66 (ID: 001002) and RNU48 (ID: 001006).

Western blotting

To extract total protein, cells were lysed in RIPA lysis buffer (ThermoFisher Scientific) supplemented with Halt Protease Inhibitor Cocktail (ThermoFisher Scientific). The concentration of the protein lysates were measured and then the lysates were boiled in Tris-Glycine SDS Sample Buffer (ThermoFisher Scientific). Equal amount of protein was separated by 4-20% Tris-Glycine gel (ThermoFisher Scientific) and then transferred onto PVDF membrane using the iBlot2 Dry Blotting System (ThermoFisher Scientific). The membrane was blocked with 5% non-fat dried skimmed milk

powder (Cell Signaling Technology) and incubated with HRP-conjugated rabbit anti-PD-L1 antibody (#51296, PD-L1 (E1L3N®) XP®, 1:1000; Cell Signaling Technology) (17, 18, 29) or primary mouse anti-β-actin (#SC-69789, 1:2000; Santa Cruz Biotechnology). Then the membrane was incubated with goat anti-mouse or anti-rabbit HRP secondary antibody (Santa Cruz Biotechnology) and protein signals were developed with the SuperSignal West Pico Chemiluminescent Substrate (ThermoFisher Scientific) using LAS4000 imager (GE Healthcare) (29).

Flow cytometry and detection of apoptosis

For the analysis of cell surface PD-L1 expression, cultured cells were harvested and re-suspended in ice-cold PBS with 1% FBS, and then cell suspensions were incubated with PE conjugated anti-human CD274 (PD-L1, B7-H1) monoclonal antibody (M1H1) (12-5983, 1:40; eBioscience, San Diego, CA, USA) (17, 29, 31) for one hour on ice in the dark. For detection of apoptotic cells, we used Annexin Ⅴ-PE/7-Amino-Actinomycin D (7-AAD) Apoptosis Detection Kit (BD Bioscience; Franklin Lakes, NJ, USA) according to the manufacturer specification. Annexin V and 7-AAD staining was measured by FACSCanto II (Becton Dickinson Bioscience, Franklin Lakes, NJ, USA) and data were analyzed with Flowjo software (TOMY Digital Biology, Tokyo, Japan).

Cell proliferation and colony formation assays

To evaluate cell proliferation, WST-cell proliferation assay using Cell Counting Kit-8 (CCK-8, DOJINDO, Kumamoto, Japan) was performed according to the manufacturer's specification. Briefly, HCT116 cells transfected with miR-148a-3p mimics or negative controls were harvested and plated at 2,000 cells in 100 μl media per well in 96 well plates. After 24, 48, 72, and 96 hours of incubation in complete medium, the cells were treated with 10 μl of the CCK-8 reagent and incubated at 37℃ for 2 hours, and then the absorbance at 450nm was measured by a microplate reader.

For the colony formation assay, transfected cells were plated at 500 cells in 6 well plates and cultured for 10 days. At the end of 10 days, the cells were fixed with fixation solution (87.5% methanol, 12.5% acetic acid) for 5 minutes and stained with 0.5% crystal violet. Colonies containing more than 50 cells were counted.

Co-culture experiments

Peripheral blood mononuclear cells (PBMCs) were purified from the fresh blood of healthy donors by using Lymphoprep (STEMCELL Technologies, Vancouver, Canada). PBMCs were stimulated with 200 IU/ml of human IL-2 (Sigma-Aldrich, Saint Louis, MO, USA) in AIM-Ⅴ medium

(ThermoFisher Scientific) for more than 7 days, in which PD-1 expression on T-cells can be forced (29, 32). IL-2 stimulated cells were co-cultured with tumor cells treated with IFN-γ and miR-148a-3p mimic at 2:1 ratio in 24 well plates. After 48 hours incubation, the population of apoptotic CD3 positive cells, T-cells, were analyzed with Annexin Ⅴ-PE/7-AAD Apoptosis Detection Kit using flow cytometry (29).

Statistical analysis

Fisher's exact test or Chi-square test was used to assess associations between categorical variables. Comparison between gene or miRNA values across groups were assessed using Mann-Whitney *U* test, or Kruskal-Wallis test with Dunn's post-hoc test, as appropriate. All statistical analyses were conducted using Graphpad Prism v6.0 (Graphpad Software, La Jolla, CA, USA). All P-values were two-sided, and P-values less than 0.05 were considered statistically significant.

Results

Identification of miR-148a-3p as a putative regulator of PD-L1

To explore the miRNA-mediated regulatory mechanisms of PD-L1 in CRC, we conducted an integrative analysis utilizing the TCGA-COAD dataset of comprehensive mRNA/miRNA-sequence combined with MMR status (n=260) (2). This approach was based on the principle that specific miRNAs with altered expression should be related to different tumor phenotypes (MMR status) and be correlated inversely with the expression of their functional target genes (PD-L1). In the TCGA dataset, PD-L1 (encoded by *CD274* gene) mRNA levels were significantly upregulated in dMMR tumors compared to pMMR tumors, as depicted in Figure 1A and reported in recent studies (33, 34). Of 47 miRNA probes showing significant negative correlation with PD-L1 expression ($P<0.0001$) (Supplementary Table S1), 19 mature miRNAs were found to be significantly decreased in dMMR tumors ($P<0.05$), as demonstrated in Figure 1A. We then tested those 19 miRNAs using a panel of 8 different sequence-based miRNA target prediction algorithms, leading to the identification of miR-148a-3p being common to 7 of 8 searches (Figure 1B). Those algorithms consistently demonstrated a putative miR-148a-3p-binding site at position 133-139 (GCACUG) in the 3'-UTR of PD-L1 mRNA (Figure 1C). We also analyzed miR-200b and miR-429, since the miR-200 family miRNAs have recently been shown to regulate PD-L1 expression by directly targeting its 3'-UTR (21). We found that miR-200b and miR-429 were each predicted to target PD-L1 by 5 of 8 programs, and that their expression levels were inversely correlated with PD-L1, irrespective of MMR status (Figure 1A-B), confirming the validity of our computational screening.

Association between miR-148a-3p, PD-L1 and MMR status

According to the recent TCGA analysis by Ock et al. (33), we also attempted to divide TCGA tumors into PD-L1^{High} or PD-L1^{Low} subgroups based on the median *CD274* mRNA expression, showing that PD-L1^{High} tumors had significantly lower levels of miR-148a-3p, than those of PD-L1^{Low} ($P<0.0001$, Figure 2A). As compared to tumors with pMMR/PD-L1^{Low}, miR-148a-3p expression was significantly decreased in pMMR/PD-L1^{High} tumors ($P<0.05$) as well as in dMMR/PD-L1^{High} tumors ($P<0.01$), and it appears that miR-148a-3p downregulation was found predominantly in dMMR/PD-L1^{High} tumors (Figure 2A). Furthermore, the inverse relationship between PD-L1 and miR-148a-3p expression was confirmed in an additional mRNA/miRNA microarray dataset of pMMR CRC by Low et al. (24), in which miR-148a-3p was significantly decreased in PD-L1^{High} tumors ($P=0.0073$) (Figure 2B). To further address the association between the expression of miR-148a-3p, PD-L1, and MMR status, we next evaluated PD-L1 protein expression in 395 samples of resected CRC specimens by IHC in the FMU cohort (Figure 2C-F). Consistent with previous IHC studies (25, 26, 28), 20 of 395 tumors (5.1%) were considered positive for tumor cell PD-L1 expression, and it was significantly enriched in dMMR tumors ($P<0.0001$, Figure 2C-E). The expression levels of miR-148a-3p were also measured by qRT-PCR using 72 tumor RNA samples isolated from FFPE tissues. We found a trend toward decreased miR148a-3p expression in PD-L1 positive and/or dMMR tumors, although this did not reach statistical significance (Figure 2F).

miR-148a-3p as a tumor suppressor in CRC

Recent reports have suggested that miR-148a-3p can work as a tumor suppressive miRNA that is frequently downregulated in CRC and other malignancies (35-37). To confirm the tumor suppressive function of miR-148a-3p *in vitro*, we used exogenous overexpression by transfecting miR-148a-3p mimic using a CRC cell line, HCT116 (Figure 3A). Indeed, forced miR-148a-3p expression exhibited significant growth suppressive effects on HCT116 cells analyzed by cell proliferation (Figure 3B) and colony formation assays (Figure 3C).

Tumor cell PD-L1 was directly regulated by miR-148a-3p

Given that PD-L1 was predicted to be a potential target of miR-148a-3p and that miR-148-3p was negatively correlated with PD-L1 expression, we next evaluated whether miR-148a-3p directly interacts with the 3'-UTR of PD-L1 mRNA. Luciferase reporter assays were performed using reporter plasmids containing either with wild-type PD-L1 3'-UTR or mutant PD-L1 3'-UTR. As shown in Figure 4A, transfection of wild-type PD-L1 3'-UTR luciferase reporter construct together with miR-148a-3p mimic into HCT116 cells significantly inhibited the luciferase reporter activity compared to that of

negative control, while this effect was reversed when the predicted 3'-UTR-biding site was mutated. This result demonstrated that PD-L1 is a direct target of miR-148a-3p. We then assessed the effect of miR-148a on the expression of PD-L1 using two CRC cell lines, including a dMMR cell line HCT116 and a pMMR cell line SW837 (Figure 4B). In both cell lines, transfection of miR-148a-3p mimic reduced PD-L1 mRNA levels measured by qRT-PCR, by approximately 59% in HCT116 cells, and 38% in SW837 cells (Figure 4C). Moreover, overexpressed miR-148a-3p also resulted in a decrease of PD-L1 protein expression by western blot analysis of whole cell lysate (Figure 4D), and in cell surface levels by flow cytometry (Figure 4E-F). On the other hand, although transfection of miR-148a-3p inhibitor could decrease miR-148a-3p levels evaluated by qRT-PCR in both cell lines (Supplementary Figure S1A), no significant change of PD-L1 expression was observed in mRNA or protein levels by qRT-PCR, western blotting and flow cytometry (Supplementary Figure S1B-E).

miR-148a-3p reduced IFN-γ-induced PD-L1 expression

It is well accepted that cell surface PD-L1 expression in tumor cells are mainly regulated by the cytokine IFN-γ secreted by immune cells in the tumor microenvironment (10-13). To confirm the effect of IFN-γ on PD-L1 expression, HCT116 and SW837 cells were treated with IFN-γ at different doses and different exposure intervals, and then PD-L1 expression on tumor cells was examined by flow cytometry. As shown in Figure 5A-B, the stimulation effect of IFN-γ on cell surface PD-L1 expression in HCT116 and SW837 was demonstrated in a dose dependent manner, and IFN-γ treatment for 48h at 10 ng/ml was used for further experiments. We next sought to determine the effect of miR-148a-3p on IFN-γ-induced PD-L1 expression. We transfected HCT116 and SW837 cell lines with miR-148a-3p mimic or negative control for 24h before IFN-γ treatment. Significantly, forced miR-148a-3p expression inhibited IFN-γ-induced PD-L1 protein expression in whole cell lysate as well as in cell surface levels (Figure 5C-E).

miR-148a-3p overexpression in tumor cells diminished T-cell apoptosis

Since miR-148a-3p could decrease PD-L1 expression on tumor cell surface, we speculated that miR-148a-3p may not only function as tumor suppressor, but also modulate immune response by inhibiting PD-L1 expressed on tumor cells. As the PD-1/PD-L1 signaling pathway is known to inhibit T-cell anti-tumor immune responses and lead T-cells to apoptosis (10), we investigated whether decreased PD-L1 expression on tumor cell by miR-148a-3p functionally reduce T-cell apoptosis using a co-culture model of cancer cells and T-cells. We harvested IL-2-activated-T-cells expressing PD-1 (29, 32), and they were then co-cultured with cancer cells transfected with miR-148a-3p mimic or negative control under treatment of IFN-γ. After 48 hours of incubation, apoptotic T-cells were measured by Annexin V/7-AAD

staining in CD3-gated population. As shown in Figure 5F-G, we found a significant decrease particularly in the percentage of late apoptotic or dead T-cells (Annexin V+/7-AAD+) when T-cells were co-cultured with HCT116 cells overexpressing miR-148a-3p (18.3±0.3 %) in comparison to that of negative control (25.4±2.5 %). A similar trend was observed in the analysis of T-cells co-cultured with SW837 cells overexpressing miR-148a-3p (Supplementary Figure S2A-B).

Discussion

The regulation of PD-L1 in cancer has been extensively investigated. The expression of PD-L1 gene is induced primarily by transcriptional mechanisms through several distinct pathways (12, 14, 15), while post-translational regulation of PD-L1 protein has been demonstrated, in which PD-L1 protein stability can be modulated by glycosylation and ubiquitination (16-18). Aside from these mechanisms, recent studies focused on post-transcriptional regulation of PD-L1 transcript targeted by miRNAs, including miR-200 and miR-34 in NSCLC (21, 22), miR-424(322) in ovarian cancer (38), and miR-152 in gastric cancer (39). Although one study reported that miR-138a-5p may target PD-L1 in CRC (40), miRNA-mediated PD-L1 expression and function in CRC remains largely unclear. The present study investigated potential miRNAs that were negatively correlated with PD-L1 expression and downregulated in MSI-H tumors using comprehensive miRNA-sequence data followed by computational target prediction algorithms. This led us to the identification of tumor suppressive miRNA, miR-148a-3p as a negative regulator of PD-L1 in CRC for the first time with our knowledge. Using CRC cell lines, we found that overexpression of miR-148a-3p reversed IFN-γ-induced PD-L1 expression in tumor cell surface that functionally correlated with diminished T-cell apoptosis in the tumor microenvironment. We thus propose a novel mechanism by which tumor immune evasion is regulated at least in part by miR-148a-3p/PD-L1 axis in CRC.

Consistent with our finding, tumor suppressive functions of miR-148a-3p have been demonstrated in many cancer types (35, 37), including CRC (36, 41). Indeed, miR-148a-3p has been reported to be downregulated in tumors, compared to their normal counterpart, which often correlated with advanced stage, where miR-148a-3p silencing was caused by DNA hypermethylation of its promotor (35, 37, 42). Decreased levels of miR-148a-3p were associated with poor clinical outcomes in a variety of cancers (43-45). Likewise, three independent studies of CRC reproducibly showed that low expression of miR-148a-3p was significantly associated with poor disease-free or cancer-specific survival in stage II and III patients (36, 41, 46). Therefore, it is clear that miR-148a-3p downregulation due to epigenetic mechanisms, can contribute to CRC progression and may serve as a prognostic biomarker for patients with stage II and III CRC. However, the involvement of miR-148a-3p in the tumor immune system has been so

far unknown. Here we provide novel evidence that miR-148a-3p plays an important role in the immunosuppressive tumor microenvironment by directly targeting PD-L1, particularly in dMMR tumors. Collectively, methylated and downregulated miR-148a-3p in tumor cells is likely to contribute not only to the tumor progression but also to the increase of tumor cell surface PD-L1 expression that can consequently help tumor cells escape from adaptive immunity.

Patients with positive PD-L1 expression in tumor cells by IHC have exhibited trends toward increased rate of responses to anti-PD-1/PD-L1 therapies across various clinical trials (47, 48). PD-L1-negative expression, however, does not imply a lack of response and those patients can still achieve clinical benefit with PD-1/PD-L1 blockade. As predictive values of PD-L1 IHC alone is insufficient for patient selection, studies are being actively conducted to develop more effective, predictive biomarkers for the PD-1/PD-L1 immunotherapy. Recently, patients with dMMR/MSI-H CRC have emerged as a distinct biomarker-defined population who could benefit from PD-1 blockade (8, 9). Despite frequent PD-L1 expression in dMMR/MSI-H CRC, not all of these patients responded to the anti-PD-1 antibody nivolumab with approximately 31% of objective response rate and 69% of disease control rate, where PD-L1 IHC was not predictive of response (9). Conversely, a small subset of pMMR/MSS CRC with or without PD-L1 expression may still benefit from immunotherapy, although it is more difficult challenge. In view of that, combination of multiple approaches to capture the immune status of CRC is considered more effective as predictive biomarkers for the response to anti-PD-1/PD-L1 therapies (48). Thus, multiple strategies, such as MMR/MSI testing, PD-L1 IHC, TIL density, neoantigens load, and immune gene signatures, combined with miR-148a-3p measurement described here may provide optimal characterization of the immune tumor microenvironment for precision cancer immunotherapy in CRC.

miRNA-based therapeutics are currently being evaluated in phase I and phase II clinical trials as new approaches for the treatment of malignancies and other diseases (49). In the treatment of cancer, therapeutic delivery of the tumor suppressive miRNA, miR-34, in which a miR-34 mimic encapsulated in lipid nanoparticles (MRX34), is the most advanced therapeutics tested in a phase I trial (ClinicalTrials.gov: NCT01829971) (49). Intriguingly, as miR-34 can directly target PD-L1 in NSCLC cell lines, the *in vivo* delivery of miR-34 via MRX34 repressed tumor PD-L1 expression in a mouse model of NSCLC. MRX34 treatment also promoted CD8+ TILs and reduced the number of exhausted CD8+PD1+ T-cells in the tumor microenvironment, indicating that MRX34 had direct effects on immune evasion (22). Since miR-148a-3p can work as a tumor suppressor and also restore T-cell function by inhibiting PD-L1, further studies are needed to investigate the possibility of miR-148a-3p replacement strategy as immunotherapy for CRC.

In conclusion, the present study demonstrated for the first time that downregulated miR-148a-3p expression was found particularly in dMMR CRC, correlating with higher levels of PD-L1 expression.

Our findings clearly suggest that miR-148a-3p suppresses IFN-γ-induced PD-L1 expressed on tumor cell surface and consequently restores T-cell viability in the tumor microenvironment. Our findings provide novel evidence that miR-148a-3p regulates immune evasion via PD-L1 and may guide development of novel cancer biomarkers as well as therapeutic interventions for CRC.

Acknowledgements

This work was supported by JSPS KAKENHI Grant Numbers 16K07146 and 16K10545. Hirokazu Okayama was supported by The Uehara Memorial Foundation.

Figure Legends

Figure 1. Downregulation of miR-148a-3p in deficient mismatch repair (dMMR) colorectal cancer (CRC), correlating inversely with programmed cell death ligand 1 (PD-L1) expression. (A) Heat map depicting samples from TCGA-COAD dataset of comprehensive mRNA/miRNA-sequence combined with MMR status (n=260). Nineteen miRNAs were shown to be significantly negatively correlated with PD-L1 (encoded by *CD274* gene) expression ($P<0.0001$) and to be significantly decreased in dMMR tumors ($P<0.05$). (B) A panel of 8 different sequence-based miRNA target prediction algorithms identifying potential miRNAs, putative biding sites of which are present in the 3'-untranslated region (UTR) of the PD-L1 mRNA. This identified miR-148a-3p as being common to 7 of 8 independent target searches. (C) The schema of PD-L1 mRNA that shows a potential binding site in the 3'-UTR of PD-L1 for miR-148a-3p.

Figure 2. Association of programmed cell death ligand 1 (PD-L1) expression with mismatch repair (MMR) status and miR-148a-3p expression in colorectal cancer (CRC). (A) The expression of miR-148-3p according to MMR status, classified as deficient (dMMR) or proficient (pMMR), combined with PD-L1 expression levels in the TCGA dataset. Tumors were divided into PD-L1^{High} or PD-L1^{Low} based on the median *CD274* mRNA expression. (B) miR-148a-3p expression in a microarray dataset of pMMR CRC in the Low cohort. (C, D) Representative images of immunohistochemistry for PD-L1 protein expression in CRC, demonstrating positive (C) and negative (D) PD-L1 staining. Bar = 250μm. (E) Association between PD-L1 protein expression by immunohistochemistry and MMR status in the Fukushima Medical University (FMU) cohort. (F) qRT-PCR analysis for miR-148a-3p expression in dMMR/PD-L1(+), pMMR/PD-L1(+), and pMMR/PD-L1(-) tumors in the FMU cohort. *$P < 0.05$, **$P < 0.01$, ***$P < 0.001$.

Figure 3. Tumor suppressive functions of miR-148a-3p in HCT116 cells. (A) Transfection of miR-148a-3p mimic increased the expression levels of miR-148a-3p analyzed by qRT-PCR. (B, C) Forced expression of miR-148a-3p in HCT116 cells analyzed by WST-cell proliferation assay (B), colony formation assay (C). *P < 0.05, **P < 0.01.

Figure 4. Programmed cell death ligand 1 (PD-L1) expression regulated by miR-148a-3p. (A) Luciferase reporter activity was analyzed after co-transfection of miR-148a-3p mimic or negative control and wild-type (wt) PD-L1 3'-UTR luciferase reporter construct or mutant (mut) construct into HCT116 cells. (B) Transfection of miR-148a-3p mimic or negative control in HCT116 and SW837 cell lines. The expression levels of miR-148a-3p were analyzed by qRT-PCR. (C, D, E, F) The expression of PD-L1 in mRNA, whole cell protein and cell surface protein levels were each evaluated by qRT-PCR (C), western blotting (D), and flow cytometry (E, F). *P < 0.05, **P < 0.01.

Figure 5. miR-148a-3p reduced interferon-γ (IFN-γ)-induced programmed cell death ligand 1 (PD-L1) in tumor cells and diminished T-cell apoptosis. (A) Dose dependent escalation of cell surface PD-L1 levels in HCT116 cells following IFN-γ stimulation. HCT116 cells were exposed to various dose of IFN-γ (0, 0.5, 1.0, 10, and 50 ng/ml) for 24 h, 48 h, or 72 h followed by flow cytometry for PD-L1. (B) HCT116 and SW837 cells were exposed to 10 ng/ml of IFN-γ for 24 h, 48 h, or 72 h. (C, D, E) HCT116 and SW837 cells were transfected with miR-148a-3p mimic or negative control for 24 h and then exposed to 10 ng/ml of IFN-γ for 48 h, and PD-L1 expression was analyzed by western blotting (C), and flow cytometry (D, E). (F, G) The proportion of CD3-gated apoptotic T-cells determined by Annexin Ⅴ/7-AAD staining. HCT116 cells transfected with miR-148a-3p or negative control were exposed to IFN-γ for 48 h, and then co-cultured with IL2-activated T-cells followed by flow cytometry. The proportion of apoptotic T-cells was considered early apoptotic (Annexin V+, 7-AAD-) and late apoptotic/dead (Annexin V+, 7-AAD+) cells. **P < 0.01.

REFERENCES

1. Siegel RL, Miller KD, Jemal A. Cancer statistics, 2016. CA Cancer J Clin. 2016;66:7-30.

2. Network TCGA. Comprehensive molecular characterization of human colon and rectal cancer. Nature. 2012;487:330-7.

3. Brenner H, Kloor M, Pox CP. Colorectal cancer. Lancet. 2014;383:1490-502.

4. Kloor M, von Knebel Doeberitz M. The Immune Biology of Microsatellite-Unstable

Cancer. Trends Cancer. 2016;2:121-33.

5. Dudley JC, Lin MT, Le DT, Eshleman JR. Microsatellite Instability as a Biomarker for PD-1 Blockade. Clin Cancer Res. 2016;22:813-20.

6. Llosa NJ, Cruise M, Tam A, Wicks EC, Hechenbleikner EM, Taube JM, et al. The vigorous immune microenvironment of microsatellite instable colon cancer is balanced by multiple counter-inhibitory checkpoints. Cancer Discov. 2015;5:43-51.

7. Topalian SL, Hodi FS, Brahmer JR, Gettinger SN, Smith DC, McDermott DF, et al. Safety, activity, and immune correlates of anti-PD-1 antibody in cancer. N Engl J Med. 2012;366:2443-54.

8. Le DT, Uram JN, Wang H, Bartlett BR, Kemberling H, Eyring AD, et al. PD-1 Blockade in Tumors with Mismatch-Repair Deficiency. N Engl J Med. 2015;372:2509-20.

9. Overman MJ, McDermott R, Leach JL, Lonardi S, Lenz HJ, Morse MA, et al. Nivolumab in patients with metastatic DNA mismatch repair-deficient or microsatellite instability-high colorectal cancer (CheckMate 142): an open-label, multicentre, phase 2 study. Lancet Oncol. 2017;18:1182-91.

10. Dong H, Strome SE, Salomao DR, Tamura H, Hirano F, Flies DB, et al. Tumor-associated B7-H1 promotes T-cell apoptosis: a potential mechanism of immune evasion. Nat Med. 2002;8:793-800.

11. Blank C, Brown I, Peterson AC, Spiotto M, Iwai Y, Honjo T, et al. PD-L1/B7H-1 inhibits the effector phase of tumor rejection by T cell receptor (TCR) transgenic CD8+ T cells. Cancer Res. 2004;64:1140-5.

12. Mimura K, Kua LF, Shiraishi K, Kee Siang L, Shabbir A, Komachi M, et al. Inhibition of mitogen-activated protein kinase pathway can induce upregulation of human leukocyte antigen class I without PD-L1-upregulation in contrast to interferon-gamma treatment. Cancer Sci. 2014;105:1236-44.

13. Taube JM, Anders RA, Young GD, Xu H, Sharma R, McMiller TL, et al. Colocalization of inflammatory response with B7-h1 expression in human melanocytic lesions supports an adaptive resistance mechanism of immune escape. Sci Transl Med. 2012;4:127ra37.

14. Chen J, Jiang CC, Jin L, Zhang XD. Regulation of PD-L1: a novel role of pro-survival signalling in cancer. Ann Oncol. 2016;27:409-16.

15. Casey SC, Tong L, Li Y, Do R, Walz S, Fitzgerald KN, et al. MYC regulates the antitumor immune response through CD47 and PD-L1. Science. 2016;352:227-31.

16. Lim SO, Li CW, Xia W, Cha JH, Chan LC, Wu Y, et al. Deubiquitination and

Stabilization of PD-L1 by CSN5. Cancer Cell. 2016;30:925-39.

17. Mezzadra R, Sun C, Jae LT, Gomez-Eerland R, de Vries E, Wu W, et al. Identification of CMTM6 and CMTM4 as PD-L1 protein regulators. Nature. 2017;549:106-10.

18. Li CW, Lim SO, Xia W, Lee HH, Chan LC, Kuo CW, et al. Glycosylation and stabilization of programmed death ligand-1 suppresses T-cell activity. Nat Commun. 2016;7:12632.

19. Berindan-Neagoe I, Monroig Pdel C, Pasculli B, Calin GA. MicroRNAome genome: a treasure for cancer diagnosis and therapy. CA Cancer J Clin. 2014;64:311-36.

20. Paladini L, Fabris L, Bottai G, Raschioni C, Calin GA, Santarpia L. Targeting microRNAs as key modulators of tumor immune response. J Exp Clin Cancer Res. 2016;35:103.

21. Chen L, Gibbons DL, Goswami S, Cortez MA, Ahn YH, Byers LA, et al. Metastasis is regulated via microRNA-200/ZEB1 axis control of tumour cell PD-L1 expression and intratumoral immunosuppression. Nat Commun. 2014;5:5241.

22. Cortez MA, Ivan C, Valdecanas D, Wang X, Peltier HJ, Ye Y, et al. PDL1 Regulation by p53 via miR-34. J Natl Cancer Inst. 2016;108.

23. Gao J, Aksoy BA, Dogrusoz U, Dresdner G, Gross B, Sumer SO, et al. Integrative analysis of complex cancer genomics and clinical profiles using the cBioPortal. Sci Signal. 2013;6:pl1.

24. Low YS, Blocker C, McPherson JR, Tang SA, Cheng YY, Wong JYS, et al. A formalin-fixed paraffin-embedded (FFPE)-based prognostic signature to predict metastasis in clinically low risk stage I/II microsatellite stable colorectal cancer. Cancer Lett. 2017;403:13-20.

25. Rosenbaum MW, Bledsoe JR, Morales-Oyarvide V, Huynh TG, Mino-Kenudson M. PD-L1 expression in colorectal cancer is associated with microsatellite instability, BRAF mutation, medullary morphology and cytotoxic tumor-infiltrating lymphocytes. Mod Pathol. 2016;29:1104-12.

26. Lee LH, Cavalcanti MS, Segal NH, Hechtman JF, Weiser MR, Smith JJ, et al. Patterns and prognostic relevance of PD-1 and PD-L1 expression in colorectal carcinoma. Mod Pathol. 2016;29:1433-42.

27. Kim JH, Park HE, Cho NY, Lee HS, Kang GH. Characterisation of PD-L1-positive subsets of microsatellite-unstable colorectal cancers. Br J Cancer. 2016;115:490-6.

28. Inaguma S, Lasota J, Wang Z, Felisiak-Golabek A, Ikeda H, Miettinen M. Clinicopathologic profile, immunophenotype, and genotype of CD274 (PD-L1)-positive colorectal carcinomas. Mod Pathol. 2017;30:278-85.

29. Thar Min AK, Okayama H, Saito M, Ashizawa M, Aoto K, Nakajima T, et al. Epithelial-

mesenchymal transition-converted tumor cells can induce T-cell apoptosis through upregulation of programmed death ligand 1 expression in esophageal squamous cell carcinoma. Cancer Med. 2018.

30. Noda M, Okayama H, Tachibana K, Sakamoto W, Saito K, Thar Min AK, et al. Glycosyltransferase gene expression identifies a poor prognostic colorectal cancer subtype associated with mismatch repair deficiency and incomplete glycan synthesis. Clin Cancer Res. 2018.

31. Mimura K, Teh JL, Okayama H, Shiraishi K, Kua LF, Koh V, et al. PD-L1 expression is mainly regulated by interferon gamma associated with JAK-STAT pathway in gastric cancer. Cancer Sci. 2018;109:43-53.

32. Kinter AL, Godbout EJ, McNally JP, Sereti I, Roby GA, O'Shea MA, et al. The common gamma-chain cytokines IL-2, IL-7, IL-15, and IL-21 induce the expression of programmed death-1 and its ligands. J Immunol. 2008;181:6738-46.

33. Ock CY, Keam B, Kim S, Lee JS, Kim M, Kim TM, et al. Pan-Cancer Immunogenomic Perspective on the Tumor Microenvironment Based on PD-L1 and CD8 T-Cell Infiltration. Clin Cancer Res. 2016;22:2261-70.

34. Bailey MH, Tokheim C, Porta-Pardo E, Sengupta S, Bertrand D, Weerasinghe A, et al. Comprehensive Characterization of Cancer Driver Genes and Mutations. Cell. 2018;173:371-85 e18.

35. Friedrich M, Pracht K, Mashreghi MF, Jack HM, Radbruch A, Seliger B. The role of the miR-148/-152 family in physiology and disease. Eur J Immunol. 2017.

36. Hibino Y, Sakamoto N, Naito Y, Goto K, Oo HZ, Sentani K, et al. Significance of miR-148a in Colorectal Neoplasia: Downregulation of miR-148a Contributes to the Carcinogenesis and Cell Invasion of Colorectal Cancer. Pathobiology. 2015;82:233-41.

37. Li Y, Deng X, Zeng X, Peng X. The Role of Mir-148a in Cancer. J Cancer. 2016;7:1233-41.

38. Xu S, Tao Z, Hai B, Liang H, Shi Y, Wang T, et al. miR-424(322) reverses chemoresistance via T-cell immune response activation by blocking the PD-L1 immune checkpoint. Nat Commun. 2016;7:11406.

39. Wang Y, Wang D, Xie G, Yin Y, Zhao E, Tao K, et al. MicroRNA-152 regulates immune response via targeting B7-H1 in gastric carcinoma. Oncotarget. 2017;8:28125-34.

40. Zhao L, Yu H, Yi S, Peng X, Su P, Xiao Z, et al. The tumor suppressor miR-138-5p targets PD-L1 in colorectal cancer. Oncotarget. 2016;7:45370-84.

41. Takahashi M, Cuatrecasas M, Balaguer F, Hur K, Toiyama Y, Castells A, et al. The clinical significance of MiR-148a as a predictive biomarker in patients with advanced colorectal cancer. PLoS One. 2012;7:e46684.
42. Xu Q, Liu LZ, Yin Y, He J, Li Q, Qian X, et al. Regulatory circuit of PKM2/NF-kappaB/miR-148a/152-modulated tumor angiogenesis and cancer progression. Oncogene. 2015;34:5482-93.
43. Xu X, Zhang Y, Jasper J, Lykken E, Alexander PB, Markowitz GJ, et al. MiR-148a functions to suppress metastasis and serves as a prognostic indicator in triple-negative breast cancer. Oncotarget. 2016;7:20381-94.
44. Li L, Liu Y, Guo Y, Liu B, Zhao Y, Li P, et al. Regulatory MiR-148a-ACVR1/BMP circuit defines a cancer stem cell-like aggressive subtype of hepatocellular carcinoma. Hepatology. 2015;61:574-84.
45. Sakamoto N, Naito Y, Oue N, Sentani K, Uraoka N, Zarni Oo H, et al. MicroRNA-148a is downregulated in gastric cancer, targets MMP7, and indicates tumor invasiveness and poor prognosis. Cancer Sci. 2014;105:236-43.
46. Tsai HL, Yang IP, Huang CW, Ma CJ, Kuo CH, Lu CY, et al. Clinical significance of microRNA-148a in patients with early relapse of stage II stage and III colorectal cancer after curative resection. Transl Res. 2013;162:258-68.
47. Nishino M, Ramaiya NH, Hatabu H, Hodi FS. Monitoring immune-checkpoint blockade: response evaluation and biomarker development. Nat Rev Clin Oncol. 2017;14:655-68.
48. Gibney GT, Weiner LM, Atkins MB. Predictive biomarkers for checkpoint inhibitor-based immunotherapy. Lancet Oncol. 2016;17:e542-e51.
49. Rupaimoole R, Slack FJ. MicroRNA therapeutics: towards a new era for the management of cancer and other diseases. Nat Rev Drug Discov. 2017;16:203-22.

Figure 1

A

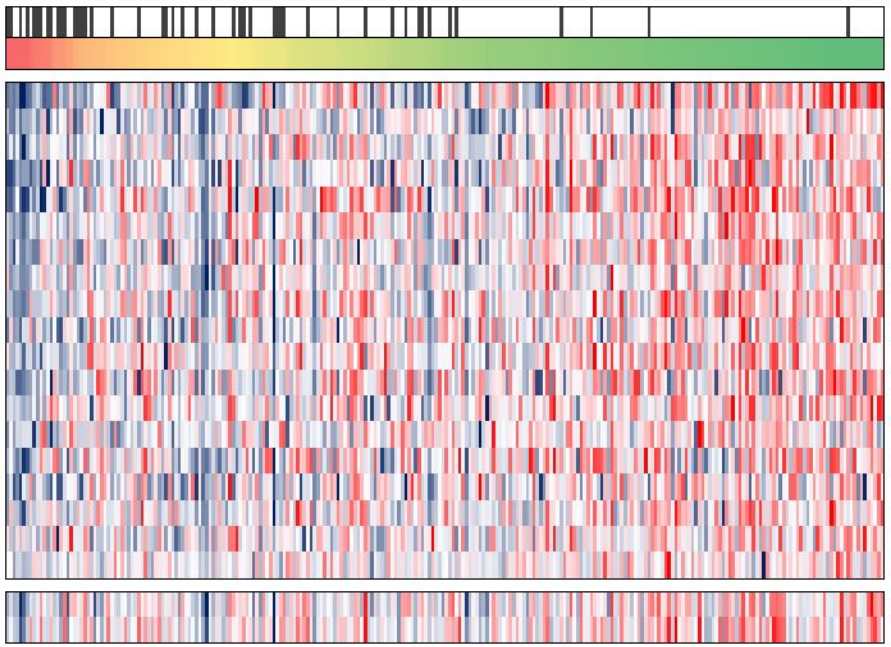

	Correlation miRs_CD274	Fold change dMMR_pMMR
hsa-mir-592	-0.498	0.14
hsa-mir-30b	-0.388	0.78
hsa-mir-362	-0.381	0.6
hsa-mir-374b	-0.35	0.24
hsa-mir-552	-0.35	0.75
hsa-mir-92a-2	-0.346	0.7
hsa-mir-95	-0.345	0.64
hsa-mir-425	-0.313	0.61
hsa-mir-92a-1	-0.313	0.81
hsa-mir-181c	-0.305	0.67
hsa-mir-224	-0.304	0.44
hsa-mir-196b	-0.301	0.42
hsa-mir-196a-1	-0.276	0.68
hsa-mir-27b	-0.267	0.88
hsa-mir-148a	-0.265	0.81
hsa-mir-181d	-0.264	0.51
hsa-mir-532	-0.258	0.75
hsa-mir-29a	-0.254	0.81
hsa-mir-101-2	-0.249	0.82
hsa-mir-429	-0.294	*n.s*
hsa-mir-200b	-0.244	*n.s*

B

ID	Accession	SUM	miRMap	RNA22	PITA	miRanda	Targetscan	microT-CDS	miRWalk	miRDB
hsa-miR-148a-3p	MIMAT0000243	7	■	■	■	■	■	■	■	
hsa-miR-27b-3p	MIMAT0000419	5	■	■	■	■			■	
hsa-miR-425-5p	MIMAT0003393	4	■		■	■	■			
hsa-miR-552-3p	MIMAT0003215	3	■	■	■					
hsa-miR-362-5p	MIMAT0000705	2	■	■						
hsa-miR-532-5p	MIMAT0002888	2	■	■						
hsa-miR-374b-5p	MIMAT0004955	1	■							
hsa-miR-92a-3p	MIMAT0000092	1		■						
hsa-miR-181d-5p	MIMAT0002821	1		■						
hsa-miR-29a-3p	MIMAT0000086	1	■							
hsa-miR-196b-5p	MIMAT0001080	1		■						
hsa-miR-196a-5p	MIMAT0000226	1		■						
hsa-miR-30b-5p	MIMAT0000420	0								
hsa-miR-181c-5p	MIMAT0000258	0								
hsa-miR-592	MIMAT0003260	0								
hsa-miR-224-5p	MIMAT0000281	0								
hsa-miR-95-3p	MIMAT0000094	0								
hsa-miR-101-3p	MIMAT0000099	0								
hsa-miR-429	MIMAT0001536	5	■		■	■	■	■		
hsa-miR-200b-3p	MIMAT0000318	5	■		■	■	■	■		

C

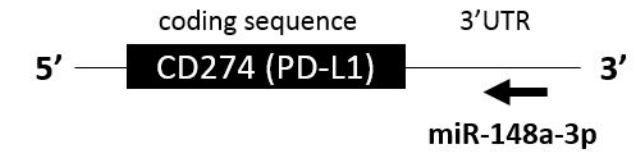

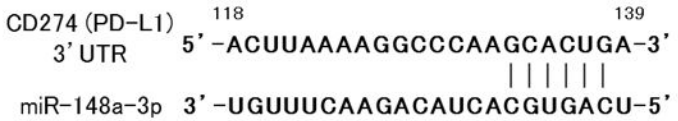

Figure 2

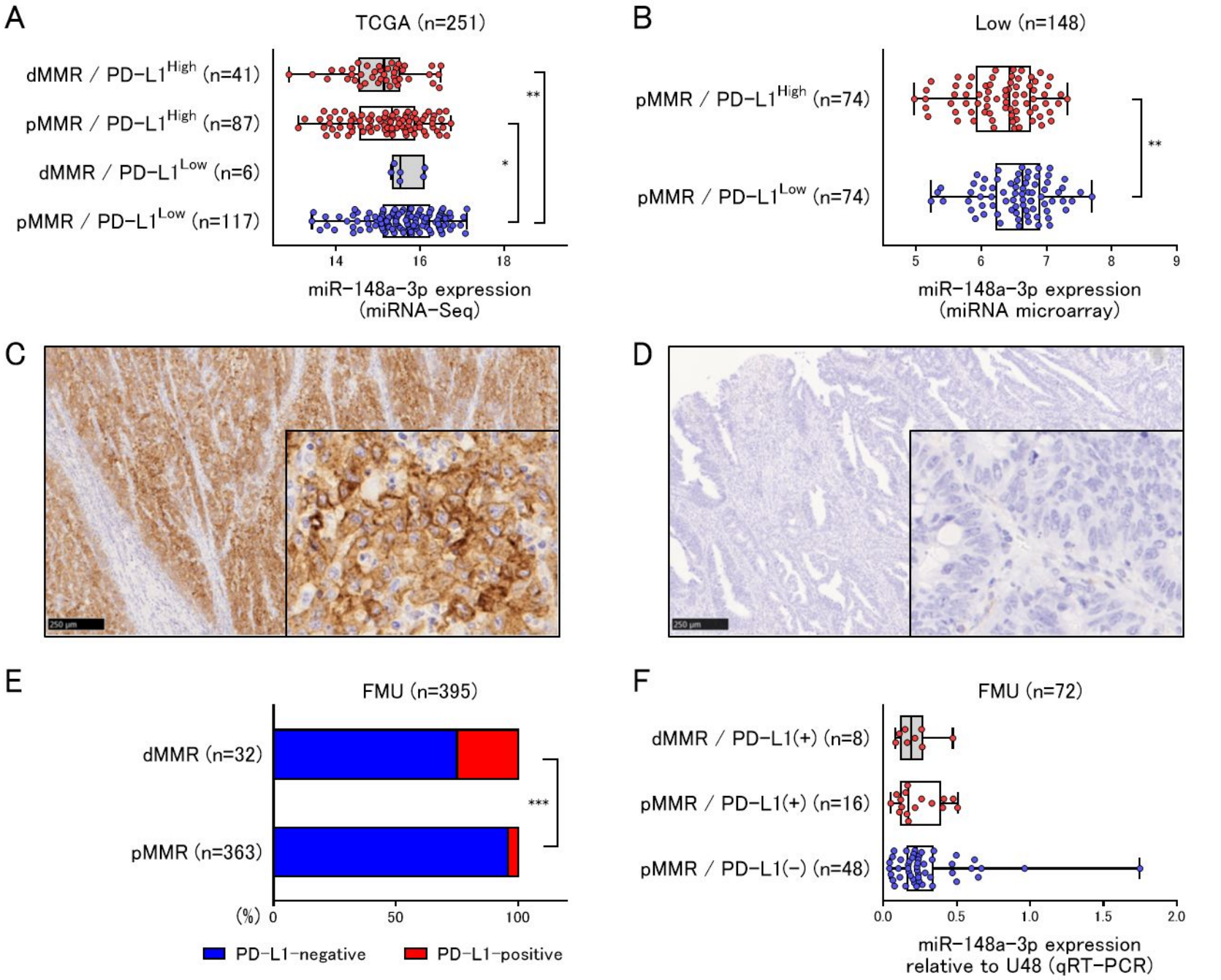
A
TCGA (n=251)
dMMR / PD-L1High (n=41)
pMMR / PD-L1High (n=87)
dMMR / PD-L1Low (n=6)
pMMR / PD-L1Low (n=117)
**
*
14
16
18
miR-148a-3p expression
(miRNA-Seq)
B
Low (n=148)
pMMR / PD-L1High (n=74)
pMMR / PD-L1Low (n=74)
**
5
6
7
8
9
miR-148a-3p expression
(miRNA microarray)
C
250 μm
D
250 μm
E
FMU (n=395)
dMMR (n=32)
pMMR (n=363)
***
(%) 0
50
100
PD-L1-negative
PD-L1-positive
F
FMU (n=72)
dMMR / PD-L1(+) (n=8)
pMMR / PD-L1(+) (n=16)
pMMR / PD-L1(-) (n=48)
0.0
0.5
1.0
1.5
2.0
miR-148a-3p expression
relative to U48 (qRT-PCR)

Figure 3

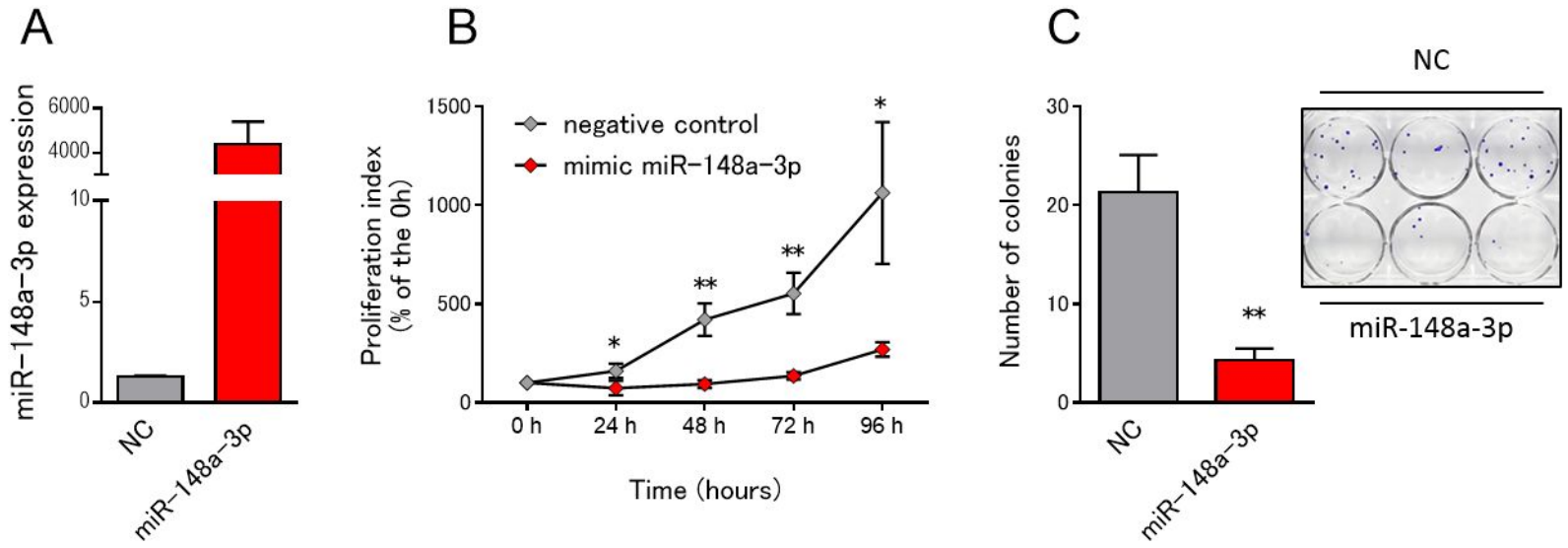
A
miR-148a-3p expression
6000
4000
10
5
0
NC
miR-148a-3p
B
Proliferation index
(% of the 0h)
1500
1000
500
0
negative control
mimic miR-148a-3p
*
**
**
*
0 h
24 h
48 h
72 h
96 h
Time (hours)
C
Number of colonies
30
20
10
0
**
NC
miR-148a-3p
NC
miR-148a-3p

Figure 4

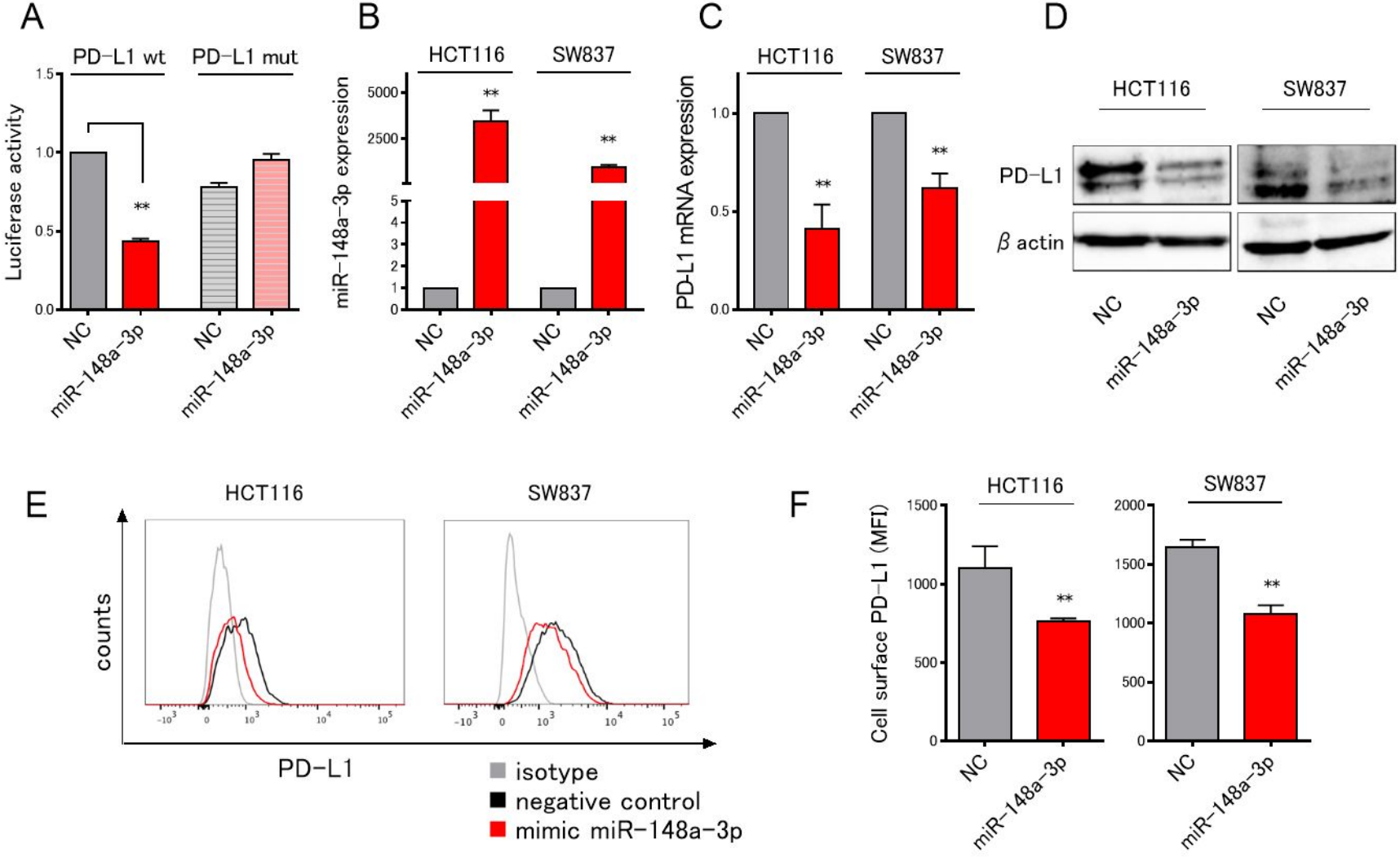
A
PD-L1 wt
PD-L1 mut
Luciferase activity
1.5
1.0
0.5
0.0
**
NC
miR-148a-3p
NC
miR-148a-3p
B
HCT116
SW837
miR-148a-3p expression
5000
2500
5
4
3
2
1
0
**
**
NC
miR-148a-3p
NC
miR-148a-3p
C
HCT116
SW837
PD-L1 mRNA expression
1.0
0.5
0.0
**
**
NC
miR-148a-3p
NC
miR-148a-3p
D
HCT116
SW837
PD-L1
β actin
NC
miR-148a-3p
NC
miR-148a-3p
E
HCT116
SW837
counts
PD-L1
isotype
negative control
mimic miR-148a-3p
F
HCT116
SW837
Cell surface PD-L1 (MFI)
1500
1000
500
0
2000
1500
1000
500
0
**
**
NC
miR-148a-3p
NC
miR-148a-3p

Figure 5

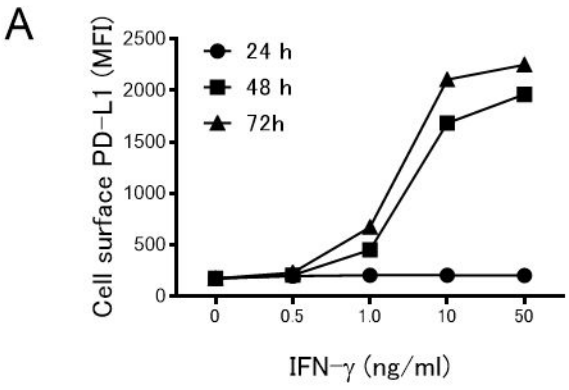
A
Cell surface PD-L1 (MFI)
2500
2000
1500
1000
500
0
24 h
48 h
72h
0
0.5
1.0
10
50
IFN-γ (ng/ml)

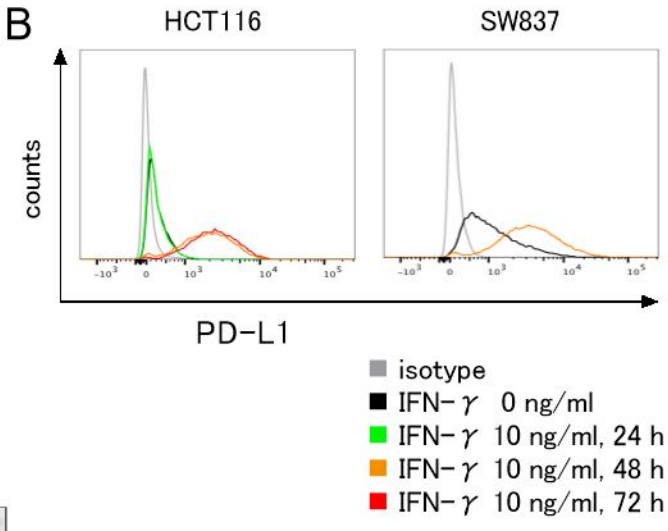
B
HCT116
SW837
counts
PD-L1
isotype
IFN-γ 0 ng/ml
IFN-γ 10 ng/ml, 24 h
IFN-γ 10 ng/ml, 48 h
IFN-γ 10 ng/ml, 72 h

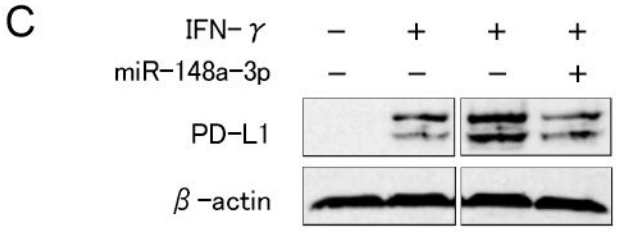
C
IFN-γ
miR-148a-3p
PD-L1
β-actin

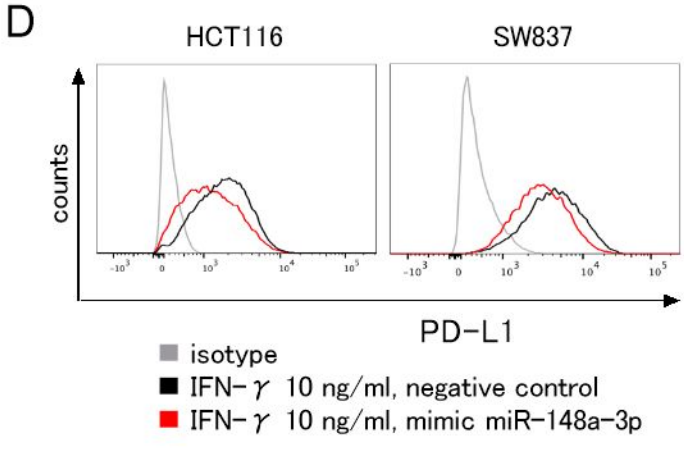
D
HCT116
SW837
counts
PD-L1
isotype
IFN-γ 10 ng/ml, negative control
IFN-γ 10 ng/ml, mimic miR-148a-3p

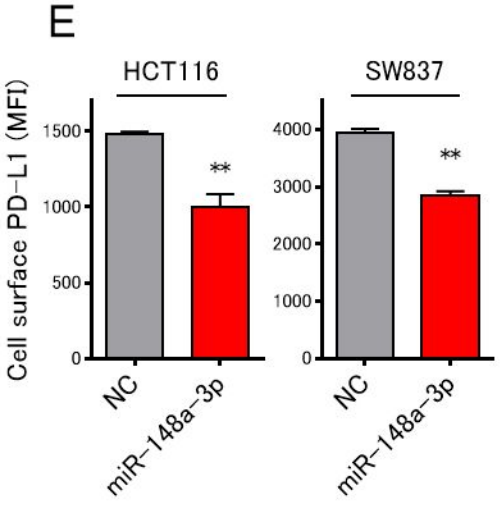
E
HCT116
SW837
Cell surface PD-L1 (MFI)
1500
1000
500
0
4000
3000
2000
1000
**
NC
miR-148a-3p

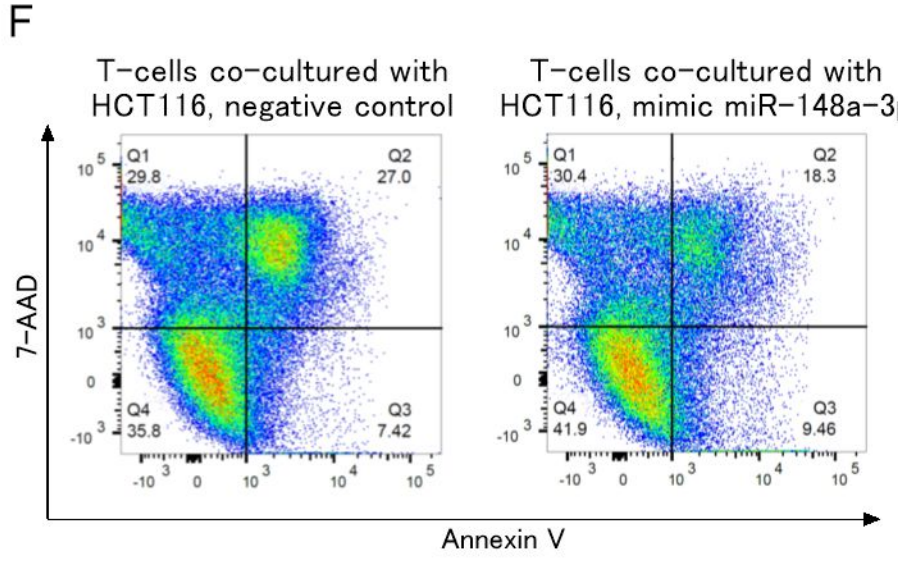
F
T-cells co-cultured with HCT116, negative control
T-cells co-cultured with HCT116, mimic miR-148a-3p
Q1 29.8
Q2 27.0
Q4 35.8
Q3 7.42
Q1 30.4
Q2 18.3
Q4 41.9
Q3 9.46
7-AAD
Annexin V

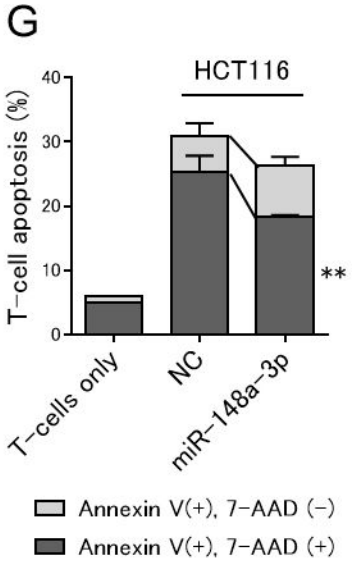
G
HCT116
T-cell apoptosis (%)
40
30
20
10
0
**
T-cells only
NC
miR-148a-3p
Annexin V(+), 7-AAD (-)
Annexin V(+), 7-AAD (+)